Chemical Engineering Journal 307 (2017) 447–455

Contents lists available at ScienceDirect

Chemical Engineering Journal

journal homepage: www.elsevier.com/locate/cej

Different influences of nanopore dimension and pH between chlorpheniramine adsorptions on graphene oxide-iron oxide suspension and particle

Chi-Min Li [a], Chun-Hu Chen [b], Wei-Hsiang Chen [a,*]

[a] Institute of Environmental Engineering, National Sun Yat-sen University, Kaohsiung 804, Taiwan, ROC
[b] Department of Chemistry, National Sun Yat-sen University, Kaohsiung 804, Taiwan, ROC

HIGHLIGHTS

- Magnetic GO-Fe_3O_4 nanocomposites were synthesized for pharmaceutical adsorption.
- Chlorpheniramine adsorption onto GO-Fe_3O_4 occurred due to a chemical adsorption.
- GO-Fe_3O_4 particles and suspension exhibited different adsorption characteristics.
- Excess nanopores enhanced chlorpheniramine adsorption on GO-Fe_3O_4 particles.
- pH variation enhanced chlorpheniramine adsorption on GO-Fe_3O_4 suspension.

GRAPHICAL ABSTRACT

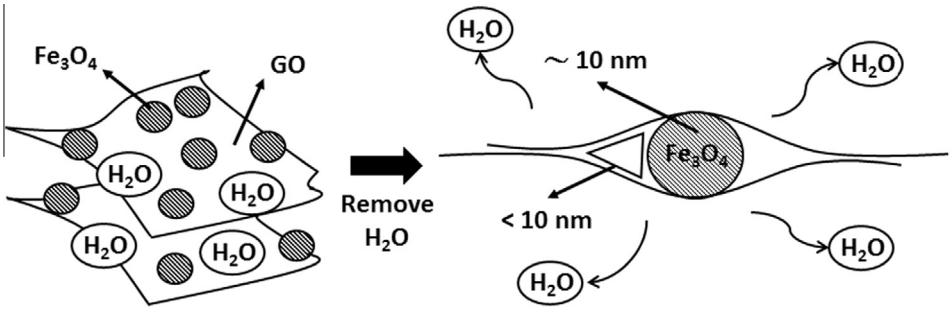

ARTICLE INFO

Article history:
Received 5 July 2016
Received in revised form 20 August 2016
Accepted 24 August 2016
Available online 25 August 2016

Keywords:
Graphene oxide
Magnetite
Chlorpheniramine
Pharmaceutical
Nanopore
pH

ABSTRACT

By synthesizing GO-Fe_3O_4 nanocomposites (graphene oxide coated with magnetite), this study investigated chlorpheniramine (a widely used pharmaceutical) adsorption on magnetic GO-Fe_3O_4, with respect to the influences of using the nanocomposite suspension or particles, mass ratios of Fe_3O_4/GO in the synthesis, pH, and contact time. GO-Fe_3O_4 was characterized by thermogravimetric analysis, X-ray diffraction, scanning electron microscopy, and Brunauer–Emmett–Teller theory. Nano-sized Fe_3O_4 anchored on GO uniformly, resulting in hybrid structures with well combination between GO and Fe_3O_4. By fitting to the pseudo 2nd-order model, chlorpheniramine adsorption onto GO-Fe_3O_4 likely occurred due to a chemical adsorption. The adsorption maximums decreased in the order: GO-Fe_3O_4 particles > GO-Fe_3O_4 suspension > activated carbon. With Fe_3O_4 changing the surface charge of GO-Fe_3O_4 suspension, pH variation enhanced chlorpheniramine adsorption on GO-Fe_3O_4 suspension. The GO-Fe_3O_4 particles exhibited a relatively better but slow chlorpheniramine adsorption. More importantly, additional nanopore volumes and surface areas were created in GO-Fe_3O_4 particles due to low Fe_3O_4 contents to more effectively capture and remove chlorpheniramine, as Fe_3O_4 crystals on the GO surface potentially prevented the compaction of GO sheets. These factors interactively affected and determined the approach of using GO for removing chlorpheniramine or other pharmaceuticals with similar molecular characteristics in wastewater treatment.

* Corresponding author.
E-mail address: whchen@mail.nsysu.eu.tw (W.-H. Chen).

http://dx.doi.org/10.1016/j.cej.2016.08.107
1385-8947/

1. Introduction

Graphene, which is a two-dimensional carbon material with exceptional electrical, mechanical, optical properties, has received great interests in various scientific areas [1–3]. As a graphene derivative, graphene oxide (GO) is an intermediate product with oxygen-containing groups on the basal plane and sheet edge [4,5]. The high specific surface area and modifiable oxygen functional groups facilitate the potential applications of GO for removing contaminants via adsorption in wastewater treatment [6,7]. Because the thickness or lateral dimension of GO is typically less than 100 nm [3], preparing magnetic GO composites is one solution to effectively remove GO from water after treatment through a magnetic field. A number of metal oxides such as TiO_2 [8], MnO_2 [9,10], and ZnO [11,12] have been applied for modification of graphene or GO. The magnetic GO nanocomposite, in which GO is coated with magnetite (Fe_3O_4), has received an intense attraction recently. The excellent magnetic properties and chemical stability make GO-Fe_3O_4 a promising and potential adsorbent for water or wastewater treatment [4,6].

Emerging contaminants (ECs), such as pharmaceuticals and personal care products (PPCPs), refer to those synthetic or naturally occurring chemicals that are not commonly monitored in the environment and cause known or suspected adverse human health and ecological effects [13,14]. These diverse substances of public and regulatory concerns are widely used for different purposes and ubiquitous in the aquatic environment [15,16]. Chlorpheniramine, 3-(4-chlorophenyl)-*N*,*N*-dimethyl-3-pyridin-2-yl-propan-1-amine, is an alkylamine antihistamine used for relieving symptoms due to upper respiratory infections and allergic conditions [17]. It is also widely used in small-animal veterinary practices. Chlorpheniramine is of concern for two main reasons. First, given its high solubility, rapid dissolution, and efficient permeability, chlorpheniramine is classified as Class 1 drug [18]. Its presences in aquatic systems have been reported, with limited information available to exactly determine the effects on the environment and ecological systems [19]. Secondly, chlorpheniramine is transformed to other more potent byproducts such as nitrosamines, which were proved to be carcinogenic and far more potent than many regulated disinfection byproducts formed during water treatment operations [20,21].

As adsorption is one of the factors in determining the overall fates of PPCPs in the environment and water treatment, the focus of this study was to elucidate the mechanism of chlorpheniramine adsorption on GO-Fe_3O_4 for its potential use to remove PPCPs in water treatment. In an early study that examined chlorpheniramine adsorption on a clay mineral montmorillonite [17], a fast adsorption, large adsorption capacity (i.e., 0.72 mmol/g), and negligible pH effect were reported, suggesting that cation exchange was the dominant mechanism and both external and internal surfaces were responsible for adsorption. However, another study, which examined copper adsorption on GO-Fe_3O_4, indicated that the adsorption was strongly dependent on pH as well as the Fe_3O_4 concentration and was dominated by inner-sphere surface complexation [22]. Given the point of zero charge (pH_{pzc}) of GO-Fe_3O_4, the surface of GO-Fe_3O_4 was positively or negatively charged at a pH below or above 4.3, respectively [22]. The pKa values of chlorpheniramine are 3.7 and 9.2 [23]. It was possible that the protonation state of chlorpheniramine and surface charge of GO-Fe_3O_4 at different pH values affected the adsorption. Besides GO-Fe_3O_4, graphene-Fe_3O_4 was used to remove rhodamine B in wastewater via adsorption and the equilibrium rapidly occurred in 30 min [6]. With the findings among different studies, this study investigated chlorpheniramine adsorption on GO-Fe_3O_4 under equilibrium and kinetic conditions, with respect to the influences of using the suspension (solution) or particles (dried powders) for adsorption, mass ratio of Fe_3O_4 to GO, solution pH, and contact time.

2. Materials and methods

2.1. Materials

Graphite powder (99.95%) was obtained from Acros Organics. Chemicals including sodium nitrate ($NaNO_3$), potassium permanganate ($KMnO_4$), hydrogen peroxide (H_2O_2), hydrogen chlorite (HCl), ferrous chloride ($FeCl_2$), ferric chloride ($FeCl_3$), and ammonium chloride (NH_4Cl) for preparation of GO-Fe_3O_4 nanocomposites were provided by Fisher Scientific. Chlorpheniramine (25 g, 99%) and bromopheniramine (100 mg, 99%) were supplied by Alfa Aesar. All experiments were conducted using deionized water buffered with sodium acetate, phosphate, or carbonate obtained from Fisher Scientific. Solution pH values were adjusted as needed using sodium hydroxide (NaOH) or sulfuric acid (H_2SO_4) (0.2 N, Fisher Scientific). All the reagents employed in this study were commercially analytical-grade and used as received without further purification.

2.2. GO-Fe_3O_4 nanocomposite preparation

GO was prepared from bulk flake graphite crystals by using the modified Hummers method [24]. One g of graphite was mixed with 0.5 g of $NaNO_3$ and 100 mL of H_2SO_4 (96%). The black solution was stirred in a flask for 30 min, followed by slow addition of 6 g of $KMnO_4$ under ice bath, turning the color of solution to dark green. After removal of the ice bath, the solution was controlled at 50 °C for 16 h. After the solution was cooled, 200 mL of deionized water and 23 mL of H_2O_2 were added into the solution to reduce the residual permanganate and manganese oxide. The solution was filtered and washed by adding 10% HCl (500 mL) and deionized water to pH 6. The solution was further exfoliated by ultra-sonication for 30 min, followed by centrifugation at 14,000 rpm for 10 min to collect the GO suspension.

GO-Fe_3O_4 nanocomposites were prepared by using different mass ratios of Fe_3O_4 to GO. S2.5, S3.7, S5, S10, and S20 denote the nanocomposites prepared with the Fe_3O_4/GO ratios of 2.5, 3.7, 5, 10, and 20, respectively. GO-Fe_3O_4 were synthesized from the GO suspension (40 mg of GO, dry weight) in 50 mL solution of $FeCl_3$ and $FeCl_2$ [25]. To prepare the S2.5, S3.7, S5, S10, and S20 nanocomposites, 100, 150, 200, 400, and 800 mg of $FeCl_3$ and 37, 56, 75, 150, and 300 mg of $FeCl_2$ were added, respectively. The solution was heated at 85 °C, and 30% ammonia solution was added to adjust the pH to 10. After being rapidly stirred for 45 min, the solution was cooled to room temperature, filtered, and rinsed with deionized water to obtain the GO-Fe_3O_4 suspension. To acquire the GO-Fe_3O_4 particles, the suspension was dried at 70 °C, followed by being ground and sieved to a 40-mesh particle size.

2.3. Batch adsorption experiments

Chlorpheniramine adsorption on GO-Fe_3O_4 was undertaken by batch adsorption experiments in 50 mL polyethylene centrifuge tubes, where stock GO-Fe_3O_4 suspension and chlorpheniramine solution were added to achieve desired experimental conditions. The experimental pH was adjusted by using NaOH or HNO_3. The suspensions were gently shaken for 24 h to achieve equilibrium or different contact times to study the kinetics. After the contact times, the solid and liquid phases were separated by using a centrifuge (4000 rpm, 15 min) and magnetic force. Liquid-liquid

extraction was used for pretreatment and gas chromatography coupled with mass spectrometry (GC/MS) was used for chlorpheniramine analysis [26]. Bromopheniramine (1 g/L, 10 μL) was spiked as the internal standard [27]. The mixture of dichloromethane and diethyl ether (the volume ratio of 4 to 1) was used to extract chlorpheniramine and bromopheniramine from the liquid phase. The extract was concentrated to 1 mL by using a rotary evaporator and nitrogen blow down.

The GC (Agilent 7890B, U.S.) was equipped with a 30 m × 0.25 mm I.D. HP-5MS capillary column with 0.25 μm film thickness. One μL of extract was injected in splitless mode. The injector temperature was 290 °C. The column temperature was programmed as follows: an initial oven temperature of 40 °C ramped at 30 °C/min to 200 °C, then 15 °C/min to 300 °C. The MS (Agilent 5977A, U.S.) was performed in the electron ionization mode and the ion source temperature was 230 °C. Data acquisition was performed with a source temperature at 350 °C. The minimum detection limit (MDL) of chlorpheniramine was approximately 1 μg/L.

2.4. Adsorption isotherm

Adsorption isotherm is a common approach for fitting experimentally-determined sorption data of pollutants in aqueous phase. Two adsorption models, namely the Freundlich (Eq. (1)) and Langmuir isotherms (Eq. (2)), were used to describe the mechanism of chlorpheniramine adsorption on GO-Fe_3O_4, as listed below [28]:

$$q = K_F C^{1/n} \quad (1)$$

$$q = \frac{q_m K_L C}{1 + K_L C} \quad (2)$$

where q and C denote the chlorpheniramine concentration adsorbed on GO [mg/kg] and dissolved in the aqueous phase [mg/L], respectively; K_F is the capacity factor [(mg/kg)/(mg/L)^n]; n is the Freundlich exponent; q_m represents the total number of surface sites per mass of sorbent [mg/g]; and K_L is the Langmuir constant [L/kg]. As mentioned above, q denotes the chlorpheniramine concentration adsorbed on GO. The chlorpheniramine adsorption onto Fe_3O_4 was not considered because our preliminary tests have shown negligible chlorpheniramine removal when only Fe_3O_4 was added in the experiments. Using only GO in the experiments is not possible as GO was difficultly separated from solution after adsorption and severely interfered the solid-phase extraction and GC/MS analysis of chlorpheniramine. In the Langmuir model, K_L is defined as the equilibrium constant of the sorption reaction and implies a constant sorbate affinity for all surface sites. The Freundlich model assumes multiple types of sorption sites acting in parallel, with each site type exhibiting a different sorption free energy and total site abundance [28].

2.5. Adsorption kinetics

The kinetics of chlorpheniramine adsorptions on GO-Fe_3O_4 suspension and particles were studied. By fitting to several kinetic models, the pseudo 2nd-order model yielded the best fit for the observed data, as the value of coefficient (R^2) were greater than 0.99 for all experiments. The pseudo 2nd-order kinetic model is expressed as follows [22]:

$$\frac{t}{q_t} = \frac{1}{k_2 q_e^2} + \frac{t}{q_e}$$

where k_2 is the 2nd-order rate constant [g/mg-min]; q_t and q_e represent the chlorpheniramine concentration adsorbed onto GO at a time t and at equilibrium [mg/g], respectively.

3. Results and discussion

3.1. Characterization of nanocomposites

Fig. 1A shows the thermogravimetric analysis (TGA) results generated on GO-Fe_3O_4 prepared with different mass ratios of Fe_3O_4 to GO. By describing the percent loss in mass of GO-Fe_3O_4 as a function of temperature, total mass losses of 34%, 27%, 23%, 16%, and 10% were observed and corresponded to the GO contents of S2.5, S3.7, S5, S10, and S20 nanocomposites, respectively. There was a gradual decrease in the GO content with more Fe_3O_4 decorated. Fig. 1B exhibits the X-ray diffraction (XRD) results of pure Fe_3O_4 and various nanocomposites. All significant diffraction peaks at 30.34°, 35.73°, 43.24°, 54.01°, 57.40°, and 62.97° of various nanocomposites matched well with the data for Fe_3O_4. The peaks were assigned to the (2 2 0), (3 1 1), (4 0 0), (4 2 2), (5 1 1) and (4 4 0) of crystal planes of Fe_3O_4 [22], and the responses became stronger with more Fe_3O_4 decorated. The nanocomposites also presented appreciable diffraction peaks at 10.3°, which indicated the inter-planar spacing due to the presence of oxides [4].

The formation of GO-Fe_3O_4 was further confirmed by scanning electron microscopy (SEM). Fig. 1C–F show the morphologies and microstructures of pure GO, S2.5, S3.7, and S5 nanocomposites, with the results of S10 and S20 nanocomposites were given in Fig. S1 in the Supporting information. In Fig. 1C, the morphology resembled thin curtains, and single or multiple GO sheets might be observed. In Figs. 1C–F and S1, nano-sized Fe_3O_4 anchored on GO uniformly, resulting in well combination between GO and Fe_3O_4 and the hybrid structures with different magnitudes. With the increasing Fe_3O_4 ratio, the sheets overlapped more and seemed to form more complex structures. The average sizes of these samples were within the range of nanometers (indicated by circles in the figure). The Van der Waals interaction between the hexagonally arrayed carbons of graphene and aromatics of organics as well as the strong π-stacking interaction between the delocalized π-electron systems of graphene and benzene rings of organics were responsible for organic adsorption onto graphene [4]. It is possible that the adsorption efficiency of chlorpheniramine onto GO-Fe_3O_4 is also affected by different sizes of nanocomposites shown in these results.

3.2. Adsorption kinetics

Fig. 2 presents the kinetic study of chlorpheniramine adsorptions on GO-Fe_3O_4 suspension and particles, respectively. Table S1 in the Supporting information shows the model applicability and associated parameter values. The high initial rates and rate constants suggested rapid removal of chlorpheniramine by GO-Fe_3O_4. Regardless of the Fe_3O_4 ratio, the estimated rate constants were relatively higher when the GO-Fe_3O_4 suspension was employed. Similar findings were shown in Fig. 2, with the equilibrium achieved in approximately 1 h and more than 3 h in the GO-Fe_3O_4 suspension and particle experiments, respectively. Based on the assumption of a pseudo 2nd-order kinetic model, chlorpheniramine adsorption onto GO-Fe_3O_4 likely occurred due to a chemical adsorption.

3.3. Adsorption isotherm

Fig. 3 illustrates the chlorpheniramine adsorptions on the GO-Fe_3O_4 suspension (Fig. 3A) or particles (Fig. 3B). The adsorbed concentration (q_e) was determined by calculating the chlorpheniramine concentration adsorbed onto GO. Additional experiments by using the activated carbon with the same mesh size were undertaken for comparison (Fig. 3B). In these experiments, the

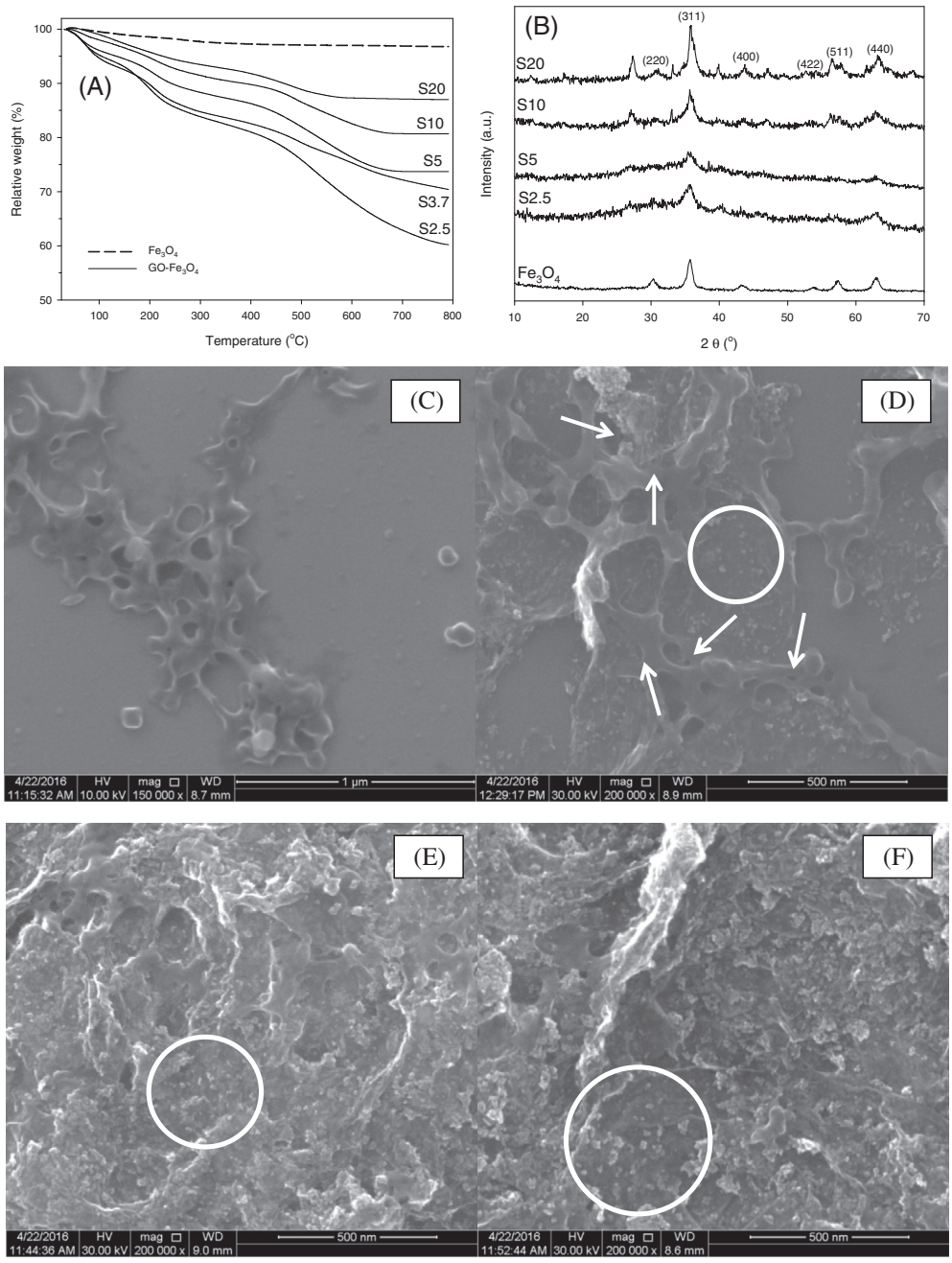

Fig. 1. (A) TGA results and (B) XRD patterns of pure Fe_3O_4 and nanocomposites prepared with different mass ratios of Fe_3O_4 to GO, and SEM results of (C) GO, (D) S2.5, (E) S3.7, and (F) S5.0 nanocomposites.

adsorbed chlorpheniramine concentrations rapidly increased and reached apparent plateaus. The adsorption maximums among three adsorbents decreased in the order: GO-Fe_3O_4 particles > GO-Fe_3O_4 suspension > activated carbon. The Freundlich and Langmuir isotherms were used to fit the observed data for investigating the adsorption capacities and kinetics (Fig. 3 and Table S2 in the Supporting information). The Freundlich model showed slightly better fits, suggesting multiple types of sorption sites acting in parallel on the surface of GO-Fe_3O_4. Given that $n < 1$ for all adsorbents, added chlorpheniramine on the surfaces of these adsorbents were bound with weaker and weaker free energies [28]. The GO-Fe_3O_4 nanocomposites, notably particles, exhibited better adsorption efficiency, as the sizes of GO-Fe_3O_4 and activated carbon were both controlled at 40 mesh size under the same experimental conditions.

3.4. Effect of the Fe_3O_4/GO mass ratio

While the GO-Fe_3O_4 suspension and activated carbon possessed similar K_F values in their Freundlich models (Table S1), the K_F values of the GO-Fe_3O_4 particles rapidly dropped with the increasing Fe_3O_4 content. Excess Fe_3O_4 on GO was likely to limit the adsorption sites for chlorpheniramine, although it increased the feasibility to remove GO from water by using the magnetic force. To investigate the influence of Fe_3O_4 proportion on chlorpheniramine adsorption, the chlorpheniramine concentrations adsorbed onto the GO-Fe_3O_4 suspension or particles at equilibrium were examined, with the nanocomposites being prepared with different mass ratios of Fe_3O_4 to GO (Fig. 4). The chlorpheniramine concentrations adsorbed by the GO-Fe_3O_4 suspension at equilibrium ranged from 168.9 to 193.4 mg/g_{GO}. The variation of Fe_3O_4 content in the

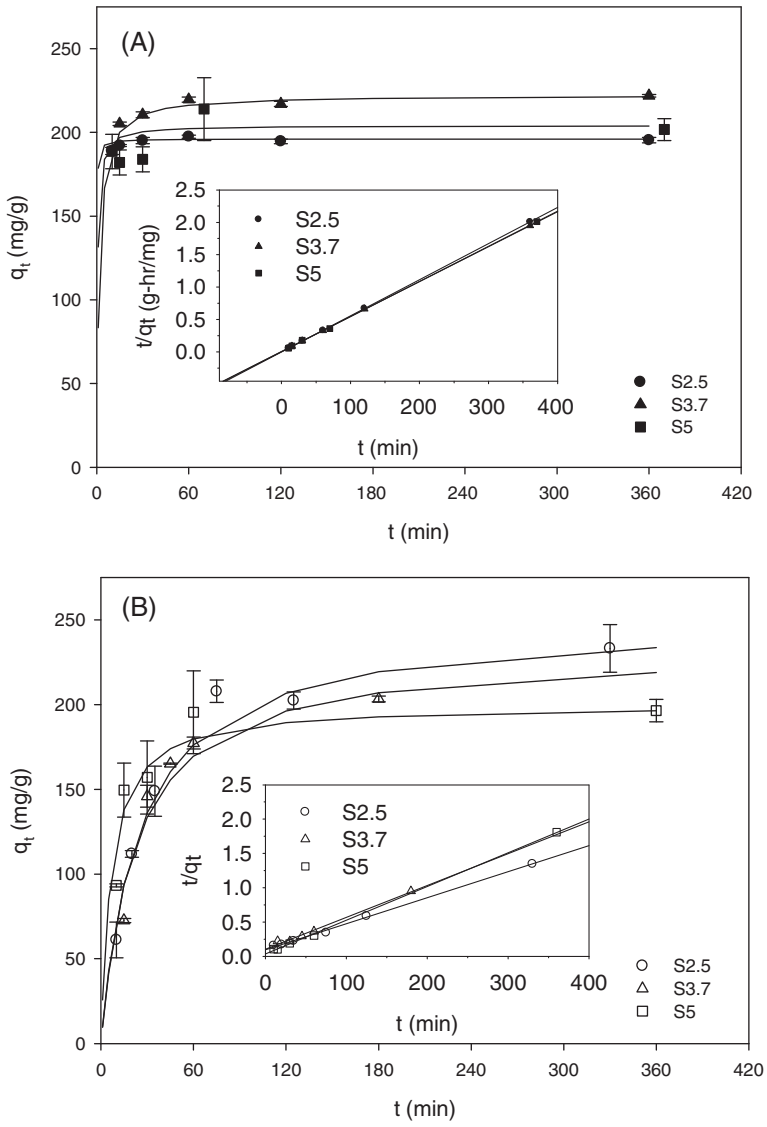

Fig. 2. Kinetics of chlorpheniramine adsorptions on GO-Fe_3O_4 (A) suspension and (B) particles. The solid line is the pseudo 2nd-order fit to the observed data. The inset is the linear plot of the kinetic curves. The initial chlorpheniramine concentration was 120 mg/L. The pH was 6.

nanocomposite did not significantly affect the adsorption capacity of GO-Fe_3O_4 suspension, implying that chlorpheniramine adsorption mainly occurred on GO and the site availability was limitedly changed. However, the chlorpheniramine concentration adsorbed on the GO-Fe_3O_4 particles gradually declined with the increasing GO-Fe_3O_4 ratio. With the Fe_3O_4/GO ratio being increased from 2.5 to 20, the adsorbed concentration dropped from 300 to 138 mg/g. Additional Fe_3O_4 decorated on GO seemed to reduce the total site abundance of GO for chlorpheniramine adsorption. A similar finding was found in a study that employed graphene-Fe_3O_4 nanocomposite for dye adsorption in wastewater treatment [4].

3.5. BET analysis

In Fig. 4, at low Fe_3O_4 to GO ratios (e.g., 2.5 or 5.0), the adsorbed chlorpheniramine concentrations in the experiments using Fe_3O_4 particles were significantly higher than those observed in the suspension experiments. Table 1 lists the surface areas, pore volumes and pore size distributions of GO-Fe_3O_4 particles analyzed by the Brunauer–Emmett–Teller (BET) theory. In the result, the nanocomposite particle with the lowest Fe_3O_4 content possessed the highest surface (221 m^2/g). Although the total pore volume was not the largest, its proportion of the micropore volume (<2 nm; 0.089 cm^3/g) to total pore volume (42%) was substantially higher than those of other nanocomposites prepared at higher Fe_3O_4 ratios. Fig. 5 shows the chlorpheniramine concentrations adsorbed on GO-Fe_3O_4 particles with different pore volumes or specific surface areas. The increase of micropore volume was positively correlated with the elevating adsorbed chlorpheniramine concentration (Fig. 5A), whereas the excess mesopore or macropore volumes lowered the adsorption capacity (Fig. 5B and C). A linear relationship was also observed between the adsorbed chlorpheniramine concentration and specific surface area (R^2 = 0.97; Fig. 5D), which was presumably due to the presence of additional micropore volume in GO-Fe_3O_4 particles prepared with low Fe_3O_4 ratios.

3.6. Influence of nanopore dimension

Fig. 6 explains the high adsorption capacity observed when GO-Fe_3O_4 particles were prepared with low Fe_3O_4 to GO ratios. After removal of water molecules at high temperatures in preparation, small amounts of Fe_3O_4 crystals possibly prevented tight com-

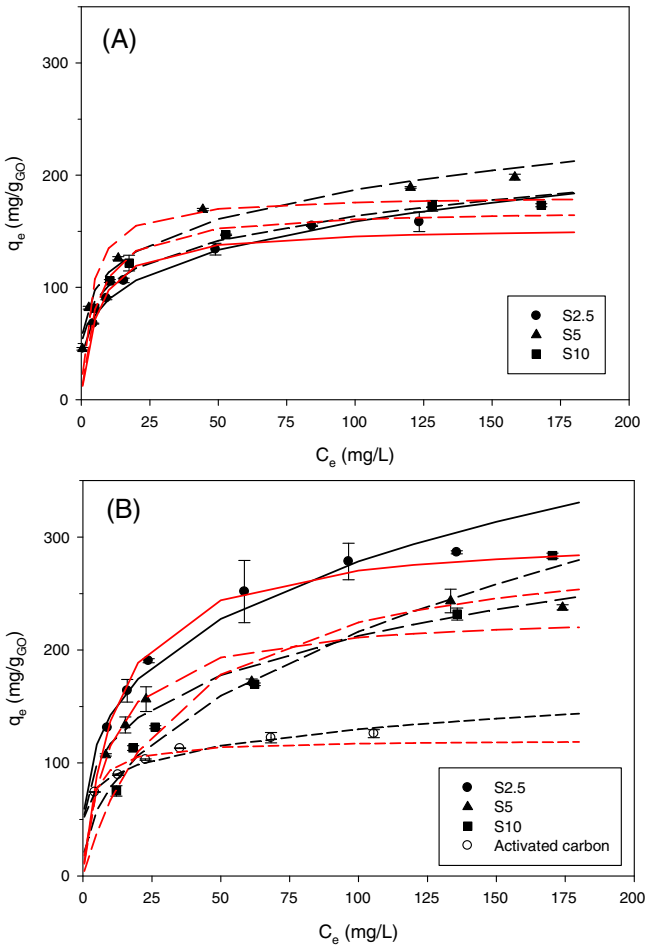

Fig. 3. Chlorpheniramine adsorptions on the GO-Fe_3O_4 nanocomposite (A) suspension and (B) particles. The black and red lines represent the Freundlich and Langmuir fits to the observed data, respectively. The solid, long-dashed, medium-dashed, and short-dashed lines denote the fits for the observed data when the nanocomposite S2.5, S5, S10, and activated carbon were used as the adsorbent, respectively. The initial chlorpheniramine concentration ranged from 10 to 200 mg/L. The experimental pH was 6 and the contact time was 24 h. (For interpretation of the references to color in this figure legend, the reader is referred to the web version of this article.)

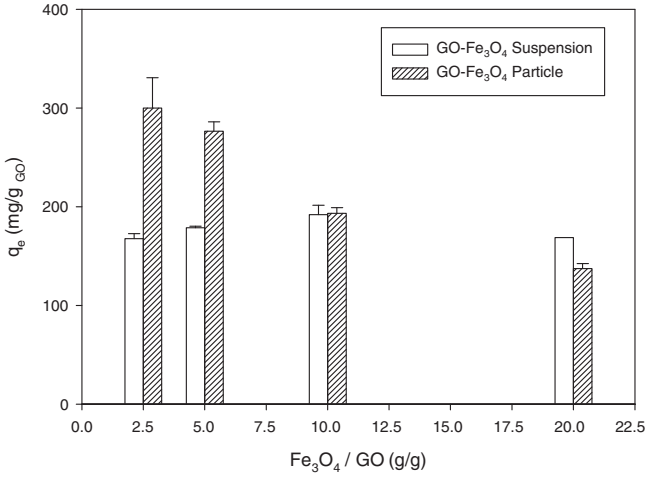

Fig. 4. Chlorpheniramine concentration adsorbed onto GO-Fe_3O_4 suspension or particles prepared with different Fe_3O_4 to GO ratios. The initial chlorpheniramine concentration was 160 mg/L. The reaction pH was 6. The contact time was 24 h.

paction of the GO sheets, assisting in forming excess nano-sized pore volumes among the GO sheets and Fe_3O_4 crystals (The possible nano-sized pores may be observed and are indicated by arrows in the SEM in Fig. 1D). Although the sizes of around 10 nm iron oxides or nanopores are far beyond the resolution limit of SEM, Scherrer equation was used to estimate the crystalline sizes of iron oxides based on (3 1 1) peak in the XRD data (Fig. 1B) [29]. The estimated crystalline sizes of iron oxides were 5.60–6.22, 5.83–6.47, 9.28–10.30, 9.40–10.44, and 10.40–11.56 nm for S2.5, S3.7, S5, S10, and S20 nanocomposite, respectively. These sizes correspond well to the sizes of nanopores obtained by the BET results. Although the crystalline sizes are not necessarily equivalent to the nanopore sizes; in this case, the nearly identical BET results further verify the particle sizes of iron oxides to be around 10 nm. The specific surface area and volume ratio of nanopore to total pore also increased at low Fe_3O_4 to GO ratios (Table 1 and Fig. 5A and D). Given the size of these nanopores, compounds such as chlorpheniramine could be more effectively captured and removed via size discrimination or capillary force. Nevertheless, in the suspension experiments, a weaker compaction among the GO layers limited the formation of excess nanopores. As more Fe_3O_4 present on the GO layers, the nanopore formation in the GO-Fe_3O_4 particle was negligible and adsorption on GO became the major mechanism for chlorpheniramine removal, creating similar adsorption capacities between the GO-Fe_3O_4 particle and suspension experiments.

3.7. Surface charge

The variations in surface charges of sorbate and sorbent are known as functions of water pH and affect adsorption. The influences could be more important when GO-Fe_3O_4 suspension was used as the adsorbent, while the pore volume and specific surface area were identified to significantly enhance chlorpheniramine adsorption on Fe_3O_4 particles. Fig. 7 depicts the zeta potential variations of pure GO and GO-Fe_3O_4 suspensions prepared with different Fe_3O_4 contents. The zeta potential of GO ranged from −40 to −55 mV. The zeta potential exceeding +30 mV or below −30 mV indicates the stability of colloidal dispersion [30]. Adding Fe_3O_4 seemed to neutralize the original electrostatic repulsion among GO sheets, as more Fe_3O_4 in the suspension resulted in less negative zeta potentials (ranging from −35 to 1.4 mV). More importantly, the point of zero charge in which GO-Fe_3O_4 exhibited a maximum coagulation and flocculation rate occurred when the pH ranged from 2 to 3 and the Fe_3O_4/GO ratio equaled to 7.5 or 15. A similar finding was observed in Fig. S2 of the Supporting information, which illustrates the GO-Fe_3O_4 suspensions prepare with different Fe_3O_4/GO mass ratios. Given the observations, the GO-Fe_3O_4 suspension was expected to resist aggregation at pH above 6.5, suggesting GO-Fe_3O_4 suspension to be employed below a neutral pH level for better separation from water after adsorption.

3.8. Effect of solution pH

Fig. 8A and B show the influences of pH on chlorpheniramine adsorption by GO-Fe_3O_4 suspension and particles, respectively. In the suspension experiments, the adsorption capacity increased from 77 mg/g at pH 4 and rose to the peak (318 mg/g) at pH 8. The charge variations of both chlorpheniramine and GO-Fe_3O_4 were possible explanations. Given the pKa values of chlorpheniramine (3.7 and 9.2), increasing the pH created a stronger electrostatic attraction between the positive chlorpheniramine and negative GO-Fe_3O_4 suspension. At pH above 9.2, chlorpheniramine became neutral, decreasing the adsorption performance with limited electrostatic attraction (the adsorption capacity dropped to

Table 1
Specific surface areas, pore volumes, and pore size distributions of nanocomposite particles prepared with different mass ratios of Fe_3O_4 to GO.

Mass ratio of Fe_3O_4 to GO	Specific surface area (m^2/g)			Pore volume			
	Total	Micro	External	Total (cm^3/g)	<2 nm[a] (%)	2–50 nm[a] (%)	>50 nm[a] (%)
2.5:1	221	51	170	0.211	42	56	2
5:1	188	28	160	0.268	18	78	4
10:1	138	20	118	0.362	9	78	13
20:1	110	14	96	0.328	6	89	5

[a] The numbers shown for <2, 2–50, and >50 nm represent the volumes of micro-, meso-, and macro-pores in proportions to the total pore volume of the nanocomposite particle.

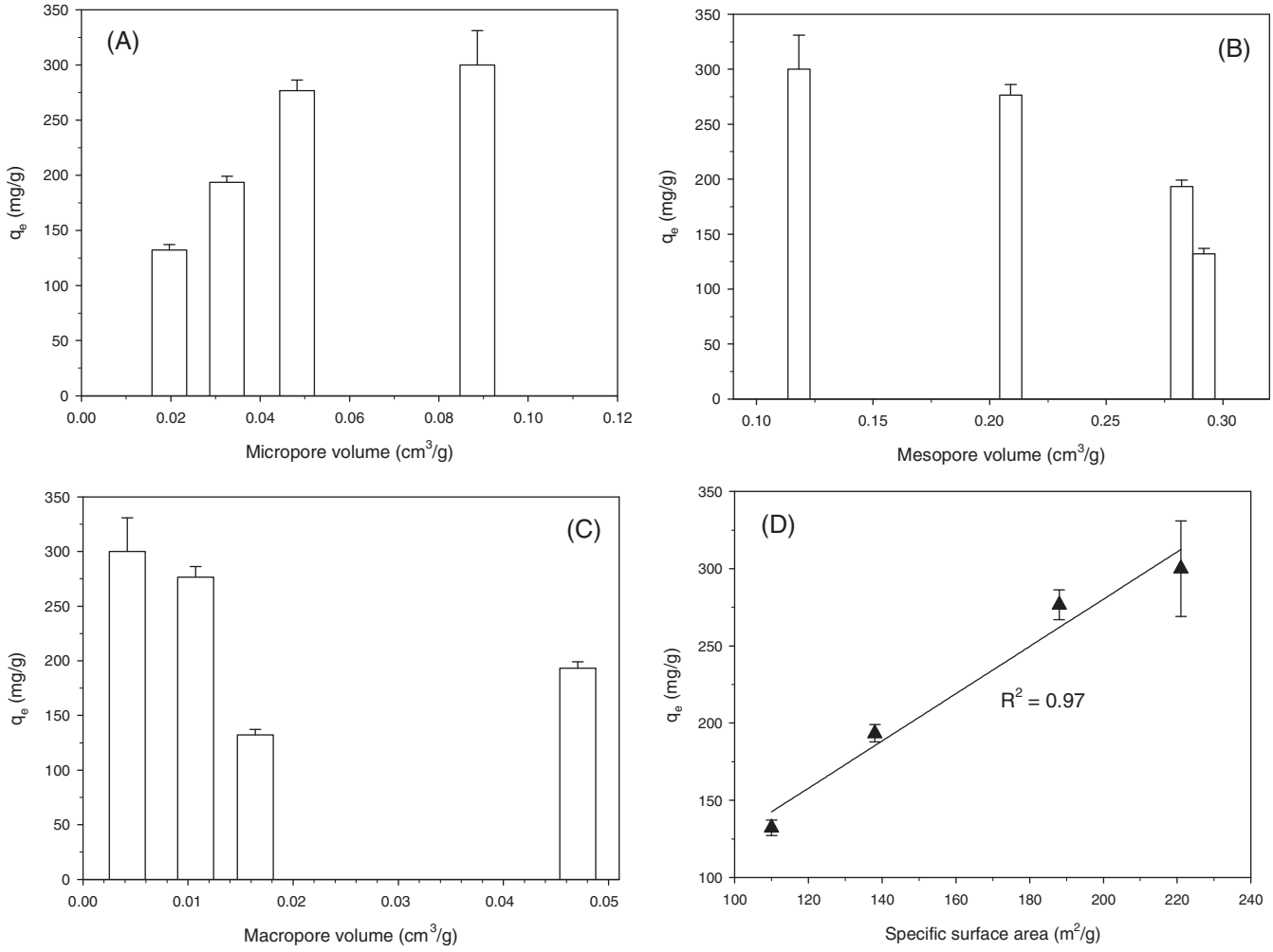

Fig. 5. Chlorpheniramine concentrations adsorbed on the GO-Fe_3O_4 nanocomposite particles with different pore volumes or specific surface areas. The micro-, meso-, and macropore volumes denote the volumes of pores with diameters less than 2 nm, between 2 and 50 nm, and larger than 50 nm, respectively.

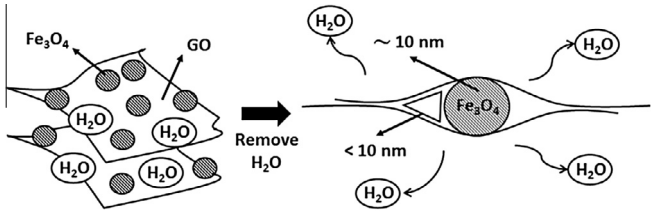

Fig. 6. Scheme of the GO/Fe oxide nanocomposite particle composition that shows the nano-sized pores (triangle) among two GO layers and iron oxide.

242 mg/g at pH 10). For GO-Fe_3O_4 particles, because the moisture had been removed at high temperatures in preparation, oxygen functional groups on GO-Fe_3O_4 were partially extruded as carbon dioxide [31]. With less important electrostatic attraction in this case, the charge of chlorpheniramine at low pH conferred its stability, inhibiting the adsorption onto GO-Fe_3O_4. At a pH above 10, chlorpheniramine became neutral and was more effectively bonded for adsorption by GO-Fe_3O_4 (the maximum adsorption capacity of 472 mg/g occurred at pH 10). Compared to the electrostatic attraction for GO-Fe_3O_4 suspension, the surface area and nano-sized pores played more important factors for chlorpheniramine adsorption on GO-Fe_3O_4 particles.

3.9. Discussion

Table 2 summarizes adsorbents which have been used for removal of chlorpheniramine and the associated performances. In

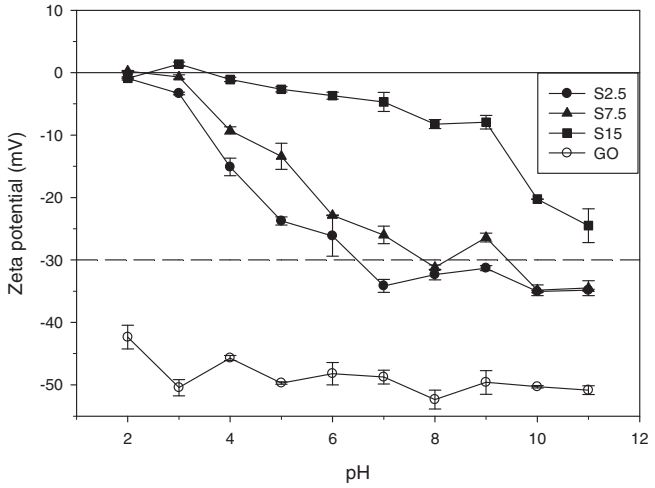

Fig. 7. Surface charge variations of GO and Fe_3O_4-GO suspensions prepared with different Fe_3O_4 contents.

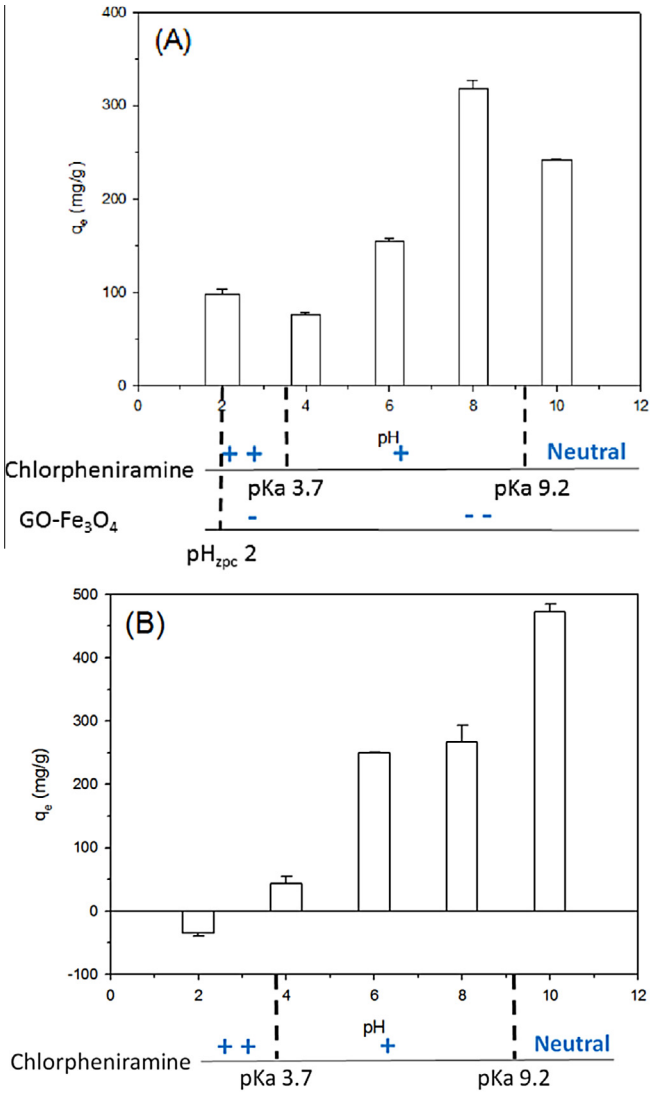

Fig. 8. Chlorpheniramine adsorption on GO-Fe_3O_4 (S2.5) (A) suspension and (B) particles at different pH values. The initial chlorpheniramine concentration was 200 mg/L. The contact time was 24 h. The lines below the figures denote the charge variations of chlorpheniramine and GO-Fe_3O_4.

Table 2
Summary of adsorbents which have been used for chlorpheniramine removal.

Adsorbent	Maximum adsorption capacity observed	pH range	Refs.
Kaolinite	7 mg/g	6–11	[33]
Phyllosilicates	17 mg/g	Alkaline	[34]
Birnessite	~80 mg/g	Alkaline	[35]
Na-Montmorillonite	176 mg/g	8–9	[34]
Ca-Montmorillonite	198 mg/g	2–9.8	[17]
GO-Fe_3O_4 suspension	317 mg/g	8	This study
GO-Fe_3O_4 particle	470 mg/g	10	This study

addition, it was reported that 75% of chlorpheniramine in deionized water could be removed by using activate carbon [32]. However, the removal efficiency declined to 40% when the background water was 90% surface water plus 10% wastewater, suggesting competitive adsorptions of other sorbates. Meanwhile, when GO was the adsorbent, four types of π bonding interactions occurred at the GO and water interface [3], with two interactions relevant to chlorpheniramine adsorption. The π-π bonding occurred between benzene rings on GO surface and C=C double bonds or benzene rings of chlorpheniramine via π-π coupling. Cation-π bonds formed between GO and easily protonated amino groups of chlorpheniramine. Similar to chlorpheniramine, many PPCPs contain these functional groups that are capable of reacting with GO. Given these specific adsorption mechanisms and high efficiency of GO compared to that of activated carbon or other adsorbents, selective adsorption of GO-Fe_3O_4 toward chlorpheniramine or other PPCPs carbon could be one topic of interest and are being investigated in our laboratory.

4. Conclusion

Chlorpheniramine adsorptions onto GO-Fe_3O_4 suspension and particles exhibited similar behaviors but were affected by different factors. By adding Fe_3O_4, the GO suspension became less stable, and therefore, removing GO-Fe_3O_4 from water after adsorption became practically feasible by using a filter or magnetic force. With the presence of Fe_3O_4 changing the surface charge of GO suspension, pH variation provided an approach to enhance chlorpheniramine adsorption. The GO-Fe_3O_4 particles exhibited a relatively better but slow chlorpheniramine adsorption. Additional nanopore volumes and surface areas were created due to low Fe_3O_4 contents to more effectively capture and remove chlorpheniramine, as Fe_3O_4 crystals on the GO surface potentially prevented the compaction of GO sheets. These factors interactively affected and determined the optimal approach of using GO for removing chlorpheniramine in water.

Acknowledgements

This research was conducted under the auspices of the Ministry of Science and Technology (MOST) under a contact number (MOST 103-2221-E-110-007-MY2). Its content are solely the responsibility of the authors and do not necessarily represent the official views of the MOST.

Appendix A. Supplementary data

Supplementary data associated with this article can be found, in the online version, at http://dx.doi.org/10.1016/j.cej.2016.08.107.

References

[1] S. Stankovich, D.A. Dikin, G.H.B. Dommett, K.M. Kohlhaas, E.J. Zimney, E.A. Stach, R.D. Piner, S.T. Nguyen, R.S. Ruoff, Graphene-based composite materials, Nature 442 (2006) 282–286.

[2] A.K. Geim, K.S. Novoselov, The rise of graphene, Nat. Mater. 6 (2007) 183–191.
[3] J. Zhao, Z. Wang, J.C. White, B. Xing, Graphene in the aquatic environment: adsorption, dispersion, toxicity and transformation, Environ. Sci. Technol. 48 (2014) 9995–10009.
[4] Y. Wu, Z. Li, J. Chen, C. Yu, X. Huang, C. Zhao, L. Duan, Y. Yang, W. Lu, Graphene nanosheets decorated with tunable magnetic nanoparticles and their efficiency of wastewater treatment, Mater. Res. Bull. 68 (2015) 234–239.
[5] J. Lee, H.R. Chae, Y.J. Won, K. Lee, C.H. Lee, H.H. Lee, I.C. Kim, J.M. Lee, Graphene oxide nanoplatelets composite membrane with hydrophilic and antifouling properties for wastewater treatment, J. Membr. Sci. 448 (2013) 223–230.
[6] L.L. Fan, C.N. Luo, M. Sun, H.M. Qiu, X.J. Li, Synthesis of magnetic betacyclodextrin-chitosan/graphene oxide as nanoadsorbent and its application in dye adsorption and removal, Colloids Surf. B 103 (2013) 601–607.
[7] Z. Yang, H. Yan, H. Yang, H.B. Li, A.M. Li, R.S. Cheng, Flocculation performance and mechanism of graphene oxide for removal of various contaminants from water, Water Res. 47 (2013) 3037–3046.
[8] H. Zhang, X. Lv, Y. Li, Y. Wang, J. Li, P25-graphene composite as a high performance photocatalyst, ACS Nano 4 (2010) 380–386.
[9] Z. Fan, J. Yan, T. Wei, L. Zhi, G. Ning, T. Li, F. Wei, Asymmetric supercapacitors based on graphene/MnO_2 and activated carbon nanofiber electrodes with high power and energy density, Adv. Funct. Mater. 21 (2011) 2366–2375.
[10] S. Chen, J. Zhu, X. Wu, Q. Han, X. Wang, Graphene oxide-MnO_2 nanocomposites for supercapacitors, ACS Nano 4 (2010) 2822–2830.
[11] K. Chung, C.-H. Lee, G.-C. Yi, Transferable GaN layers grown on ZnO-coated graphene layers for optoelectronic devices, Science 330 (2010) 655–657.
[12] Y. Zhang, H. Li, L. Pan, T. Lu, Z. Sun, Capacitive behavior of graphene-ZnO composite film for supercapacitors, J. Electroanal. Chem. 634 (2009) 68–71.
[13] T. Heberer, Occurrence, fate, and removal of pharmaceutical residues in the aquatic environment: a review of recent research data, Toxicol. Lett. 131 (2002) 5–17.
[14] C.G. Daughton, T.A. Ternes, Pharmaceuticals and personal care products in the environment: agents of subtle change?, Environ Health Perspect. 107 (1999) 907–938.
[15] A.Y.C. Lin, C.F. Lin, Y.T. Tsai, H.H.H. Lin, J. Chen, X.H. Wang, T.H. Yu, Fate of selected pharmaceuticals and personal care products after secondary wastewater treatment processes in Taiwan, Water Sci. Technol. 62 (2010) 2450–2458.
[16] Y.C. Guo, S.W. Krasner, Occurrence of primodone, carbamazepine, caffeine, and precursors for N-nitrosodimethylamine in drinking water sources impaired by wastewater, J. Am. Water Resour. Assoc. 45 (2009) 58–67.
[17] Z. Li, P.-H. Chang, J.-S. Jean, W.-T. Jiang, H. Hong, Mechanism of chlorpheniramine adsorption on Ca-montmorillonite, Colloids Surf. A 385 (2011) 213–218.
[18] J.M. Custodio, C.-Y. Wu, L.Z. Benet, Predicting drug disposition, absorption/elimination/transporter interplay and the role of food on drug absorption, Adv. Drug Deliv. Rev. 60 (2008) 717–733.
[19] J. Roberts, A. Kumar, J. Du, C. Hepplewhite, D.J. Ellis, A.G. Christy, S.G. Beavis, Pharmaceuticals and personal care products (PPCPs) in Australia's largest inland sewage treatment plant, and its contribution to a major Australian river during high and low flow, Sci. Total Environ. 541 (2016) 1625–1637.
[20] J. Lv, L. Wang, Y. Song, Y. Li, N-nitrosodimethylamine formation from ozonation of chlorpheniramine: influencing factors and transformation mechanism, J. Hazard. Mater. 299 (2015) 584–594.
[21] R.Q. Shen, S.A. Andrews, NDMA formation from amine-based pharmaceuticals – impact from prechlorination and water matrix, Water Res. 47 (2013) 2446–2457.
[22] J. Li, S. Zhang, C. Chen, G. Zhao, X. Yang, J. Li, X. Wang, Removal of Cu(II) and fulvic acid by graphene oxide nanosheets decorated with Fe_3O_4 nanoparticles, ACS Appl. Mater. Interfaces 4 (2012) 4991–5000.
[23] C. Chen, S. Leavey, S.W. Krasner, I.H. Suffet, Applying polarity rapid assessment method and ultrafiltration to characterize NDMA precursors in wastewater effluents, Water Res. 57 (2014) 115–126.
[24] M. Hirata, T. Gotou, S. Horiuchi, M. Fujiwara, M. Ohba, Thin-film particles of graphite oxide 1: high-yield synthesis and flexibility of the particles, Carbon 42 (2004) 2929–2937.
[25] M.Z. Kassaee, E. Motamedi, M. Majdi, Magnetic Fe_3O_4-graphene oxide/polystyrene: fabrication and characterization of a promising nanocomposite, Chem. Eng. J. 172 (2011) 540–549.
[26] P.J. Phillips, S.G. Smith, D.W. Kolpin, S.D. Zaugg, H.T. Buxton, E.T. Furlong, Method Description, Quality Assurance, Environmental Data, and other Information for Analysis of Pharmaceuticals in Wastewater-Treatment-Plant Effluents, Streamwater, and Reservoirs, 2004–2009, 2010.
[27] R.A. Moreno, D. Oliveira-Silva, C.E. Sverdloff, B.C. Borges, P.A.R. Galvinas, R.B. Astigarraga, N.C. Borges, Determination of chlorpheniramine in human plasma by HPLC–ESIMS/MS: application to a dexchlorpheniramine comparative bioavailability study, Biomed. Chromatogr. 24 (2010) 774–781.
[28] R.P. Schwarzenbach, P.M. Gschwend, D.M. Imboden, Environmental Organic Chemistry, John Wiley & Sons Inc., New Jersey, USA, 2003.
[29] C. Roth, M. Goetz, H. Fuess, Synthesis and characterization of carbon-supported Pt-Ru-WOx catalysts by spectroscopic and diffraction methods, J. Appl. Electrochem. 31 (2001) 793–798.
[30] B. Konkena, S. Vasudevan, Understanding aqueous dispersibility of graphene oxide and reduced graphene oxide through pK(a) measurements, J. Phys. Chem. Lett. 3 (2012) 867–872.
[31] W. Xia, Y. Wang, R. Bergstrasser, S. Kundu, M. Muhler, Surface characterization of oxygen-functionalized multi-walled carbon nanotubes by high-resolution X-ray photoelectron spectroscopy and temperature-programmed desorption, Appl. Surf. Sci. 254 (2007) 247–250.
[32] D. Hanigan, J. Zhang, P. Herckes, S.W. Krasner, C. Chen, P. Westerhoff, Adsorption of N-nitrosodimethylamine precursors by powdered and granular activated carbon, Environ. Sci. Technol. 46 (2012) 12630–12639.
[33] G.C. Lv, L.M. Wu, Z.H. Li, L.B. Liao, M.T. Liu, Binding sites of chlorpheniramine on 1:1 layered kaolinite from aqueous solution, J. Colloid Interface Sci. 424 (2014) 16–21.
[34] G.C. Lv, L. Liu, Z.H. Li, L.B. Liao, M.T. Liu, Probing the interactions between chlorpheniramine and 2:1 phyllosilicates, J. Colloid Interface Sci. 374 (2012) 218–225.
[35] C. Xia, G.C. Lv, L.F. Mei, K.N. Song, Z.H. Li, X.Y. Wang, X.B. Xing, B. Xu, Removal of chlorpheniramine from water by birnessite, Water Air Soil Pollut. 225 (2014).